IEEE Access
Multidisciplinary | Rapid Review | Open Access Journal

Received March 3, 2020, accepted March 23, 2020, date of publication April 3, 2020, date of current version April 20, 2020.

Digital Object Identifier 10.1109/ACCESS.2020.2985309

Hot-Carriers' Effect on the Performance of Organic Schottky Diodes

LING-FENG MAO
School of Computer and Communication Engineering, University of Science and Technology Beijing, Beijing 100083, China
e-mail: mail_lingfeng@aliyun.com

This work was supported by the National Natural Science Foundation of China under Grant 61774014.

ABSTRACT Because thermionic emission or tunneling occurs when carriers overcome or tunneling through the barrier for any Schottky diode, hot carriers caused by the applied electric field can enhance carrier thermionic emission or carrier tunneling. An analytical and physical organic diode current equation that includes hot-carriers effect on the diode current equation has been proposed. When organic diode current equation has the same mathematical expression as Shockley diode current equation does, hot-carrier effects in organic semiconductor diodes can be a physical origin of the ideality factor and can reduce the barrier height for both band-like conduction mechanism and hopping conduction mechanism. The voltage-dependent ideality factor and temperature-dependent ideality factor predicted by the proposed model agree well with experimental data of organic semiconductor diodes reported in the literature. The proposed model can also physically explain the experimental relation between the ideality factor and the effective barrier height. The proposed model is useful in better physically understanding the carrier transport in organic semiconductor diodes. It also benefits to better optimize the organic semiconductor diode performance by tuning material properties.

INDEX TERMS Organic Schottky diode, organic semiconductor, Schottky barrier, thermionic emission.

I. INTRODUCTION

Organic semiconductor-based devices have been widely studied due to their flexibility, large area, and low-cost processability [1]–[18]. Organic semiconductor diodes are one of the basic building blocks of the modern semiconductor industry and organic semiconductors are still in the developmental phase. The exponential behavior of organic diode current can be described as the Shockley diode current equation or thermionic emission current [1]–[8]. Different values of the ideality factors and Schottky barrier heights under different applied voltage and temperature have been reported [1]–[8]. Therefore, understanding the physics behind the operation of organic semiconductor diodes (the mechanisms governing charge transport and charge recombination) is helpful to improve the performance of organic semiconductor-based devices. A debatable issue occurs because there are different charge transport mechanisms in organic semiconductor-based devices [9]–[18]. A conventional band like description [9] and hopping incoherently from molecule to molecule [10] in organic semiconductor-based devices have been reported.

The associate editor coordinating the review of this manuscript and approving it for publication was Jenny Mahoney.

The Shockley diode current equation is believed to give the current-voltage characteristic of an ''idealized'' diode, which is widely used [19]. At the same time, Schottky diodes are also named as hot-carrier diodes, it implies that the thermionic emission current gives the main contribution to the total diode current. But in most studies of these Schottky diodes (for example, Ref. 6), the authors did not mention any hot-carrier effect in their papers. It means that hot-carriers effects in Schottky diodes are worthy of further study. An ideality factor has been introduced into the Shockley diode current equation for a measure of how the Shockley diode current equation or the current equation of Schottky diodes follows the ideal diode current equation [19]. Based on the consideration of the ideality factor in the Shockley diode current equation, the experimental data of diode current can be described by the Shockley diode equation. Therefore, the physical origin and the physical understanding of the ideality factor in the Shockley diode current equation lacks.

On can note that thermionic emission current in semiconductor diodes or thermally induced flow of carriers over a potential-energy and the effects of the applied electric field on the carrier velocity have been neglected in the conventional semiconductor diode current equation [19]. In the former studies, it has been found that hot-carriers effects

caused by the applied electric field can have a large effect on the performance of semiconductor devices. [20]–[33]. Hot-carriers effects in GaN-based devices can decrease its channel electron density [20] and decrease its source-drain current [21], [22]. Hot-carriers effects in the graphene-based devices can reduce Schottky barrier height [23], shift its spectra of Raman photo- and electro-luminescence [24], be a physical origin of the ideality factor [25]. Hot carriers in organic semiconductor-based devices can reduce their effective activation energy [26]. Hot-carriers effects in silicon based-devices can reduce the barrier height [27], change its tunneling current [28], decrease its channel electron density [29], increase its gate leakage current [30], [31], change its surface potential [32], affect its capacitance [33], [34], be a physical origin of the ideality factor of Shockley diode current equation [35].

The above results demonstrate that hot-carriers effects in organic semiconductor-based devices should be considered in modeling their performance. It also implies that hot-carriers effects in organic semiconductor-based devices on carrier transport should be considered. The purpose of this paper is to develop a physical understanding of how hot-carriers effects in organic semiconductor-based devices affect their performance. For example, the ideality factor in the diode current equation of organic semiconductor-based devices and the reduction in the Schottky barrier height and the reason why they depend on temperature, the applied voltage, etc. In other words, discussing the physical origin of the ideality factor and the reduction in the Schottky barrier height of the organic semiconductor-based devices can shed some light on how to physically understand and improve their performance. The proposed model can explain the experimental relation of how the ideality factor and the reduction in the Schottky barrier height of the organic semiconductor diodes depend on temperature, the doping concentration, and the applied voltage. The proposed model through its simplicity and analytic nature gives a possible physical origin of the ideality factor of organic semiconductor-based devices.

II. THEORY

One can note that band like carriers transport in organic semiconductor-based devices has been found in conducting crystalline organic semiconductors [9]. The conduction band (π^* orbital) or the lowest unoccupied molecular orbital (LUMO) and upper state of the valence band (π orbital) and corresponds to the highest occupied molecular orbital (HOMO) exist in organic semiconductors. The charge transport takes place in π bonding and antibonding orbitals or other terms in HOMO and LUMO levels. The charged carriers usually transport by hopping from one molecule to another. Different charge transport mechanisms in organic semiconductors have also been reported [11]. This leads to a debatable issue. Charge carrier mobility is an important fundamental parameter in bulk-limited conduction organic semiconductors, where transport phenomena can be dominated by band transport or hopping transport. The carrier mobility is defined as the proportionality constant of the drift velocity to the electric field strength. In other words, carriers in an organic semiconductor-based device will get an additional drift when an electric field is applied. For a Schottky junction, there are five basic transport processes (thermionic emission, tunneling, recombination, diffusion of electrons, and diffusion of holes) under the forward bias [19]. A diode current requires that carriers overcome the Schottky barrier of organic semiconductor-based devices. It means that tunneling and thermionic emission will occur at the Schottky barrier. One can note that the width of the space charge region in an organic semiconductor diode is usually large (in the unit of μm), which means that the tunneling current is very small and can be neglected. This is the reason why only the thermionic emission is considered in this article. In a word, diode current due to tunneling can be neglected for the case of the diode with a large space charge width, whereas tunneling may come into the picture for explaining the current transport in addition to thermionic emission for the case of the diode with a narrow space charge width (for example, a highly doped diode). Based on the above discussion, the band like carriers transport has been firstly discussed in the following. Then, the localized carriers transport in organic semiconductor-based devices will be discussed based on phenomenology.

For a metal-organic semiconductor contact at thermal equilibrium shown in Figure 1, the built-in potential for n-type organic semiconductor and p-type organic semiconductor can be written as

$$q\psi_{BI} = q\phi_B - q\phi_n = q\left(\phi_m - \chi\right) - q\phi_n \tag{1}$$

$$q\psi_{BI} = q\phi_B - q\phi_p = E_g - q\left(\phi_m - \chi\right) - q\phi_p \tag{2}$$

where E_g is the bandgap of the organic semiconductor, $q\phi_B$ is the barrier height, $q\phi_m$ is the work function of the metal, $q\chi$ is the electron affinity of the organic semiconductor, q is the electron charge, ϕ_n is the Fermi potential from the conduction-band edge in n-type organic semiconductor ($q\phi_n = E_C - E_F = -k_B T_L \ln(N_D/N_C)$), ϕ_p is the Fermi potential from the conduction-band edge in p-type organic semiconductor ($q\phi_n = E_F - E_V = -k_B T_L \ln(N_A/N_V)$), E_F is the Fermi level, N_C is the effective density of states in the conduction band of the organic semiconductor, N_V is the effective density of states in the valence band of the organic semiconductor, E_C is the bottom of conduction-band of the organic semiconductor, and E_V is the top of the conduction band of the organic semiconductor. With the complete ionization assumption ($\frac{d^2\psi}{dx^2} = \frac{qN_D}{\varepsilon_s}$ and $\frac{d^2\psi}{dx^2} = -\frac{qN_A}{\varepsilon_s}$, the electric field in the depletion region of n-type organic semiconductor and p-type organic semiconductor via integrating the Poisson's equation (the metal-organic semiconductor interface is set as $x = 0$) is

$$F\left(x\right) = -\frac{qN_D}{\varepsilon_s}\left(W_{Dn} - x\right) \tag{3}$$

$$F\left(x\right) = \frac{qN_A}{\varepsilon_s}\left(W_{Dp} - x\right) \tag{4}$$

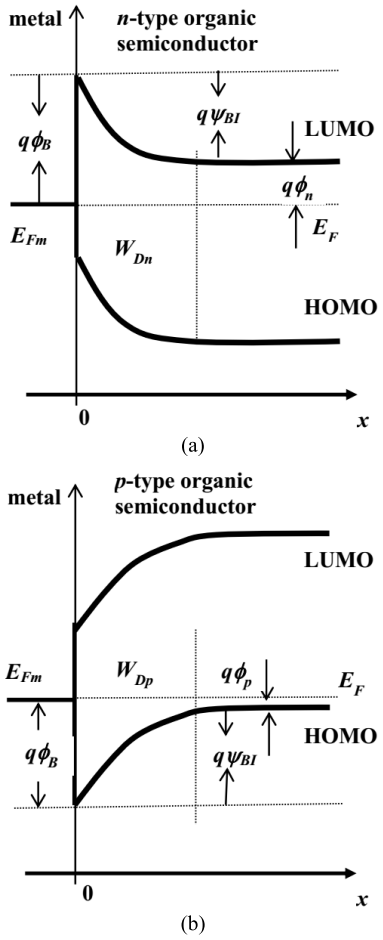

FIGURE 1. The band diagram of a metal-n-type organic semiconductor contact (a) metal-p-type organic semiconductor contact (b) at thermal equilibrium.

where W_{Dp} is the width of the depletion region in the p-type organic semiconductor at thermal equilibrium, W_{Dn} is the width of the depletion region in the n-type organic semiconductor at thermal equilibrium, N_D is the donor density of the organic semiconductor, N_A is the acceptor density of the organic semiconductor, and ε_s is the dielectric constant of the organic semiconductor. When the potential in the inside of organic semiconductor is set as zero, the potential of n-type organic semiconductor and p-type organic semiconductor is

$$\psi_i(x) = \frac{qN_D}{2\varepsilon_s}(x - W_{Dn})^2 \tag{5}$$

$$\psi_i(x) = -\frac{qN_A}{2\varepsilon_s}\left(x - W_{Dp}\right)^2 \tag{6}$$

For organic Schottky junction $\psi_i(x)|_{x=0} = \psi_{BI}$ at thermal equilibrium, $W_{Dn} = \sqrt{\frac{2\varepsilon_s\psi_{BI}}{qN_D}}$ and $W_{Dp} = \sqrt{-\frac{2\varepsilon_s\psi_{BI}}{qN_A}}$. When a uniform forward applied electric field F (Let $F = V/W_D$, in other words. V applied to a metal-organic semiconductor junction is the voltage drop across the total depletion region at non- equilibrium, thus the electric field $F(x, V)$ in the depletion region of n-type organic semiconductor and p-type organic semiconductor

$$F(x) = -\frac{qN_D}{\varepsilon_s}(W_{Dn} - x) + \frac{V}{W_{Dn}} \tag{7}$$

$$F(x) = \frac{qN_A}{\varepsilon_s}\left(W_{Dp} - x\right) - \frac{V}{W_{Dp}} \tag{8}$$

And thus the potentials of the n-type organic semiconductor and the p-type organic semiconductor are

$$\psi_i(x) = \frac{qN_D}{2\varepsilon_s}(x - W_{Dn})^2 + \frac{V}{W_{Dn}}(W_{Dn} - x) \tag{9}$$

$$\psi_i(x) = -\frac{qN_A}{2\varepsilon_s}\left(x - W_{Dp}\right)^2 - \frac{V}{W_{Dp}}\left(W_{Dp} - x\right) \tag{10}$$

Eq. 7 and Eq. 8 (Eq. 9 and Eq. 10) demonstrate that the depletion region in the metal-organic semiconductor at thermal equilibrium will be divided into a depletion region and an accumulation region after a forward applied electric field or a forward voltage is applied to the organic diode. The depletion region means a negative electric field in an n-type organic semiconductor and a positive electric field in a p-type organic semiconductor. The accumulation region means a positive electric field for n-type organic semiconductors and a negative electric field for p-type organic semiconductors. The boundaries between the depletion region and accumulation region of n-type organic semiconductor and p-type organic semiconductor occur at

$$x_B = W_{Dn} - \frac{\varepsilon_s V}{qN_D W_{Dn}} \tag{11}$$

$$x_B = W_{Dp} - \frac{\varepsilon_s V}{qN_A W_{Dp}} \tag{12}$$

It means that the accumulation region (from x_B to W_{Dn} or W_{Dp}) will occur when the organic Schottky diode is applied to a forward electric field or a forward voltage. One can note that the carriers will be accelerated in the accumulation region of an organic semiconductor diode under the forward voltage. The average net electric field across such an accumulation region of the n-type organic semiconductor and the p-type organic semiconductor can be obtained as

$$F_{ave} = \frac{\int_{x_B}^{W_{Dn}} F(x)dx}{W_{Dn} - x_B} = \frac{V}{2W_{Dn}} = \frac{V}{2\sqrt{\frac{2\varepsilon_s\psi_{BI}}{qN_D}}} \tag{13}$$

$$F_{ave} = \frac{\int_{x_B}^{W_{Dp}} F(x)dx}{W_{Dn} - x_B} = -\frac{V}{2W_{Dn}} = -\frac{V}{2\sqrt{\frac{2\varepsilon_s\psi_{BI}}{qN_A}}} \tag{14}$$

The thermal emission current should be the most possible current conduction mechanism for a Schottky diode. And the diode current density from the organic semiconductor into the metal is [19]

$$J_{OS\to M} = \int_{q(\psi_{BI}-V)}^{\infty} qv_i dn \tag{15}$$

where $v_{\rm i}$ is the carrier velocity along the transport direction in the s region before over the barrier. According to the above discussion, the carriers in organic Schottky diodes under an applied forward electric field will get a drift velocity in the accumulation region before they enter into the depletion region. If the carrier velocity before entering the region ($0 \leq x \leq W_{Dn}$, or $0 \leq x \leq W_{Dp}$) is assumed to be v_x, the carrier velocity before over the junction barrier or the depletion region can be written as

$$v_i = \sqrt{n_e} v_x = v_x + \mu_e F_{ave} = v_x + \mu_e \frac{V}{2W_{Dn}} \tag{16}$$

$$v_i = \sqrt{n_h} v_x = v_x + \mu_h F_{ave} = v_x + \mu_h \frac{V}{2W_{Dp}} \tag{17}$$

where μ_e is electron mobility of the organic semiconductor, μ_h is hole mobility of the organic semiconductor, n_e and n_h are factors for electrons and holes, that are related to the drift velocity. Thus, Eq. 15 can be rewritten as

$$J_{OS\to M} = \int_{q(\psi_{BI}-V)}^{\infty} q\sqrt{n_e} v_x dn \tag{18}$$

One can note that organic semiconductors are practically insulators [11]. However the organic semiconductor is a semiconductor or insulator or conductor, if its energy dispersion can be treated as a parabolic band, The electron state volume of all three-dimensional materials in k-space between energy E and $E + \Delta E$ can be obtained as $g_{3D}(E) = \frac{k^2}{\pi^2 \frac{\partial E}{\partial k}} = \frac{1}{2\pi^2}\left(\frac{2m^*}{\hbar^2}\right)^{3/2} E^{1/2}$. The three-dimensional density of electrons in the parabolic band materials can be obtained $dn = \frac{1}{2\pi^2}\left(\frac{2m^*}{\hbar^2}\right)^{3/2} E^{1/2} \frac{1}{1+\exp\left(\frac{E-E_F}{k_B T}\right)} dE$. Integrating Eq.18 for electrons and holes,

$$J_{OS\to M} = q\frac{\sqrt{n_e} m_e^* (k_B T_L)^2}{2\pi^2\hbar^3} e^{-\frac{q\phi_n}{k_B T_L}} e^{-\frac{m_e^* v_{0x}^2}{2k_B T_L}} \tag{19}$$

$$J_{OS\to M} = q\frac{\sqrt{n_h} m_h^* (k_B T_L)^2}{2\pi^2\hbar^3} e^{-\frac{q\phi_p}{k_B T_L}} e^{-\frac{m_h^* v_{0x}^2}{2k_B T_L}} \tag{20}$$

where $k_{\rm B}$ is the Boltzmann constant, $T_{\rm L}$ is the device temperature or lattice temperature, m_e^* is the effective electron mass, m_h^* is the effective electron mass, $\hbar$ is the reduced Planck's constant. Therefore, the minimum velocity required in the transport direction to surmount the potential barrier region or the depletion region of an organic semiconductor is given by $\frac{1}{2}m_e^* v_i^2 = \frac{1}{2}m_e^* n_e v_{0x}^2 = q(\psi_{bi} - V)$ for electrons and $\frac{1}{2}m_h^* v_i^2 = \frac{1}{2}m_h^* n_h v_{0x}^2 = q(\psi_{bi} - V)$ for holes. Here, v_{0x} is the minimum velocity for thermionic emission along the transport direction in organic Schottky diode at $x = W_{Dn}$ or $x = W_{pn}$. It means that $\frac{1}{2}m^* v_{0x}^2 = \frac{q(\psi_{bi}-V)}{n_e}$. Thus, thermionic current for electrons and holes in organic Schottky diodes can be written as

$$J_{OS\to M} = q\frac{\sqrt{n_e} m_e^* (k_B T_L)^2}{2\pi^2\hbar^3} e^{-\frac{\left(q\phi_n + \frac{q\psi_{bi}}{n_e}\right)}{k_B T_L}} e^{\frac{qV}{k_B T_L n_e}} \tag{21}$$

$$J_{OS\to M} = q\frac{\sqrt{n_h} m_h^* (k_B T_L)^2}{2\pi^2\hbar^3} e^{-\frac{\left(q\phi_p + \frac{q\psi_{bi}}{n_h}\right)}{k_B T_L}} e^{\frac{qV}{k_B T_L n_h}} \tag{22}$$

Comparing the above equations with the Shockley diode equation and the conventional thermionic emission current equation, $n_{\rm e}$ and $n_{\rm h}$ should be equivalent to the ideality factors n. $n_{\rm e}$ and $n_{\rm h}$ in the proposed model are correlated with the drift velocities according to Eq. 16 and Eq.17. There is no such expression in the conventional thermionic emission current equation because the drift velocities have not been considered in the conventional thermionic emission theory. There is no such expression in the conventional thermionic emission current equation because the drift velocities have not been considered in the conventional thermionic emission theory. When hot-carriers effects have been included in the thermionic emission theory, a factor that is correlated to the drift velocity in the thermionic emission current equation has been obtained. It can change the Schottky barrier height. It can also introduce such a factor in the mathematic formal of the exponential dependent term related to the applied voltage in the diode current equation. Such ideality factors in the diode current equation of organic semiconductor-based devices physically origin from carriers becoming hot (an additional drift velocity caused by the applied voltage). So does the effective Schottky barrier that can also be concluded from the above diode current equation of organic semiconductor-based devices. According to Eq.21 and Eq. 22, the effective barrier height of the n-type organic semiconductor diodes and the p-type organic Schottky diodes can be written as

$$\begin{aligned} \phi_{BE} &= q\phi_n + \frac{q\psi_{bi}}{n_e} \\ \phi_{BE} &= q\phi_p + \frac{q\psi_{bi}}{n_h} \end{aligned} \tag{23}$$

According to the above discussion, the ideality factors in the diode current equations of the n-type organic semiconductor and the p-type organic semiconductor can be physically determined as

$$\begin{aligned} \sqrt{n_e} &= \frac{v_i}{v_{0x}} = 1 + \mu_e \frac{V}{2W_{Dn} v_{0x}} = 1 + \mu_e \frac{V}{2\sqrt{\frac{2\varepsilon_s \psi_{BI}}{qN_D}} v_{0x}} \\ &= 1 + \mu_e \frac{V}{2\sqrt{\frac{2\varepsilon_s (q(\phi_m - \chi) - q\phi_n)}{q^2 N_D}} v_{0x}}) \\ &= 1 + \mu_e \frac{V}{2\sqrt{\frac{2\varepsilon_s (q(\phi_m - \chi) + k_B T_L \ln(N_D/N_C))}{q^2 N_D}} v_{0x}} \end{aligned} \tag{24}$$

$$\begin{aligned} \sqrt{n_h} &= \frac{v_i}{v_{0x}} = 1 + \mu_h \frac{V}{2W_{Dp} v_{0x}} = 1 + \mu_h \frac{V}{2\sqrt{\frac{2\varepsilon_s \psi_{BI}}{qN_A}} v_{0x}} \\ &= 1 + \mu_h \frac{V}{2\sqrt{\frac{2\varepsilon_s (E_g - q(\phi_m - \chi) - q\phi_p)}{q^2 N_A}} v_{0x}} \\ &= 1 + \frac{0.5\mu_h V}{\sqrt{\frac{2\varepsilon_s (E_g - q(\phi_m - \chi) + k_B T_L \ln(N_A/N_V))}{q^2 N_A}} v_{0x}} \end{aligned} \tag{25}$$

Eq. 25 and Eq. 26 clearly shows that the ideality factor diode current equation of organic semiconductor-based

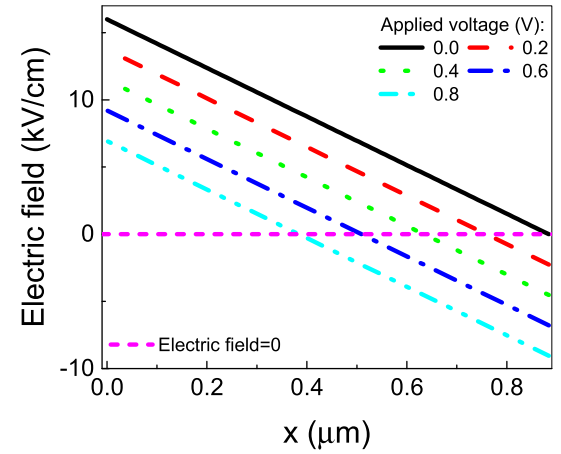

(a)

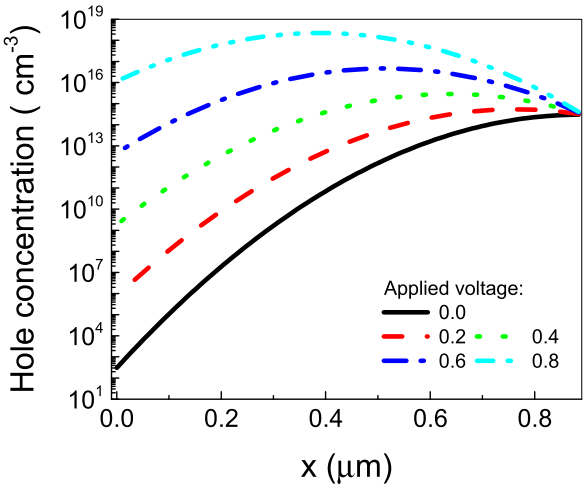

(b)

FIGURE 2. (a) The electric field (b) the hole concentration in an organic semiconductor with N_A of 3 × 10^{14} cm^{-3}at the temperature of 300 K under different forward voltage.

devices can be modulated by the work function of the metal, temperature, the applied voltage, the doping density, the carrier mobility, the electron affinity, the dielectric constant of an organic semiconductor.

In the following, temperature-dependent ideality factor, voltage-dependent ideality factor, and temperature-dependent effective barrier height in organic semiconductor-based devices will be discussed in detail. For simplicity, only *n*-type organic semiconductors will be analyzed in the following. For a *p*-type organic semiconductor Schottky diode, a similar mathematical derivation process can be performed.

Firstly, the temperature-dependent ideality factor will be discussed. For band electrons in an organic semiconductor of a diode, $\mu \sim (T_L)^{-\frac{3}{2}}$ and to $\mu \sim (T_L)^{-2}$ at $k_BT_L \leq 2t$ and $k_BT_L \leq 2t$ with $t = 143$ meV, and a rather flat metallic-like power-law behavior $\mu \sim (T_L)^{-\frac{1}{2}}$ for the random diffusion of fully incoherent states $\mu \sim (T_L)^{-\frac{1}{2}}$ [9]. For $\mu \sim (T_L)^{-\frac{3}{2}}$, we can assume $\mu = A(T_L)^{-\frac{3}{2}}$ (A is the fit parameter) under $-k_BT_L \ln\left(\frac{N_D}{N_C}\right) < q(\phi_m - \chi)$, the ideality factor in such organic semiconductor diode under one order Taylor expansion is

$$\begin{aligned}\sqrt{n_e} &= D + ET_L^{-\frac{3}{2}}\left(1 + \frac{1}{2}FT_L\right) \\ &= D + \frac{1}{2}FET_L^{-\frac{1}{2}} + ET_L^{-\frac{3}{2}} \\ &= D + \frac{1}{2}FE\left(T_L^{-\frac{1}{2}}\right) + E\left(T_L^{-\frac{1}{2}}\right)^3 \end{aligned} \tag{26}$$

where $D = 1$, $E = \frac{AV}{2v_{0x}\sqrt{\frac{2\varepsilon_S q(\phi_m-\chi)}{q^2N_D}}}$, and $F = \frac{k_B \ln\frac{N_D}{N_C}}{q(\phi_m-\chi)}$.

For $\mu \sim (T_L)^{-2}$, we can assume $\mu = A(T_L)^{-2}$ under $-k_BT_L \ln\left(\frac{N_D}{N_C}\right) < q(\phi_m - \chi)$, the ideality factor in such organic semiconductor diode under one order Taylor expansion is

$$\begin{aligned}\sqrt{n} = \lambda &= D + ET_L^{-2}\left(1 + \frac{1}{2}FT_L\right) \\ &= D + \frac{1}{2}FET_L^{-1} + ET_L^{-2} \end{aligned} \tag{27}$$

For $\mu \sim (T_L)^{-\frac{1}{2}}$, we can assume $\mu = A(T_L)^{-\frac{1}{2}}$ under $-k_BT_L \ln\left(\frac{N_D}{N_C}\right) < q(\phi_m - \chi)$, the ideality factor in such organic semiconductor diode under one order Taylor expansion is

$$\begin{aligned}\sqrt{n} = \lambda &= D + ET_L^{-\frac{1}{2}}\left(1 + \frac{1}{2}FT_L\right) \\ &= D + \frac{1}{2}FET_L^{\frac{1}{2}} + ET_L^{-\frac{1}{2}} \end{aligned} \tag{28}$$

For a Schottky diode with disorder organic semiconductor [10], $\mu \sim e^{-\frac{B}{T_L}}$ when the traps are homogeneously dispersed and $\mu \sim e^{-\frac{B}{(T_L)^2}}$ for a Gaussian-type disorder (B is the fit parameter). For $\mu \sim e^{-\frac{B}{T_L}}$, we can assume $\mu = Ae^{-\frac{B}{T_L}}$ under $-k_BT_L \ln\left(\frac{N_D}{N_C}\right) < q(\phi_m - \chi)$, the ideality factor in such organic semiconductor diode under one order Taylor expansion is

$$\begin{aligned}\sqrt{n} = \lambda &= D + Ee^{-\frac{B}{T_L}}\left(1 + \frac{1}{2}FT_L\right) \\ &\approx D + E\left(1 - \frac{B}{T_L}\right)\left(1 + \frac{1}{2}FT_L\right) \\ &= \left(D + E - \frac{1}{2}EBF\right) - EBT_L^{-1} + \frac{1}{2}EFT_L^1 \end{aligned} \tag{29}$$

For $\mu \sim e^{-\frac{B}{(T_L)^2}}$, we can assume $\mu = Ae^{-\frac{B}{(T_L)^2}}$ under $-k_BT_L \ln\left(\frac{N_D}{N_C}\right) < q(\phi_m - \chi)$, the ideality factor in such organic semiconductor diode under one order Taylor expansion is

$$\begin{aligned}\sqrt{n} = \lambda &= D + Ee^{-\frac{B}{(T_L)^2}}\left(1 + \frac{1}{2}FT_L\right) \\ &\approx D + E\left(1 - \frac{B}{(T_L)^2}\right)\left(1 + \frac{1}{2}FT_L\right)\end{aligned}$$

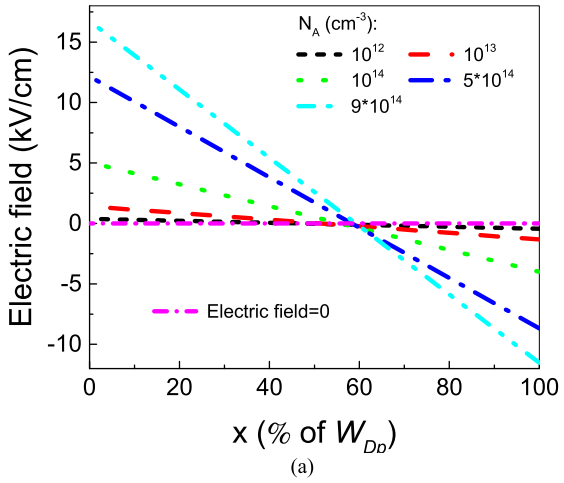

(a)

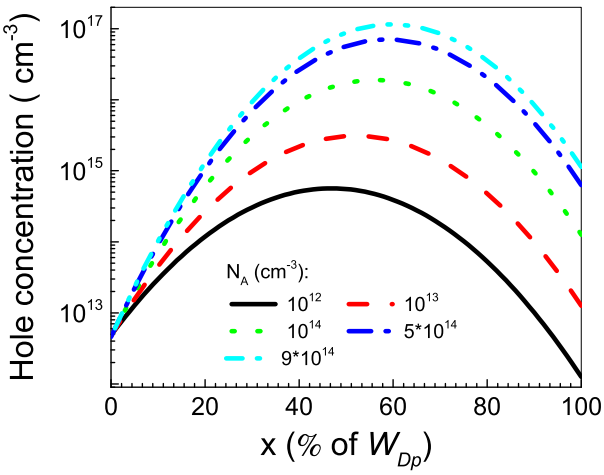

(b)

FIGURE 3. (a) The electric field (b) the hole concentration in an organic semiconductor with a forward voltage of 0.6 V at the temperature of 300 K for different N_A.

$$= (D+E) - EBT_L^{-2} - \frac{1}{2}EFBT_L^{-1} + \frac{1}{2}EFT_L^{1} \quad (30)$$

Secondly, the voltage-dependent ideality factor in organic semiconductor diodes will be discussed. Note that the carrier density exponentially decreases with its energy according to Fermi-Dirac distribution, the energy around the required minimum energy ($\frac{1}{2}m_e^* v_{0x}^2 = q(\psi_{BI} - V)$) will give a main contribution to the thermionic emission current. If $\psi_{BI} > V$, Eq. 25 under one-order Taylor expansion can be rewritten as

$$\begin{aligned}\sqrt{n} &= 1 + \mu \frac{V}{2\sqrt{\frac{2\varepsilon_s \psi_{BI}}{qN_D}} v_{0x}} \\ &= 1 + \mu \frac{V}{2\sqrt{\frac{4\varepsilon_s \psi_{BI}}{m^* N_D}}} \sqrt{\psi_{BI} - V} \\ &\approx 1 + \mu \frac{V}{2\sqrt{\frac{4\varepsilon_s}{\psi_{BI} N_D m^*}}} \left(1 + \frac{V}{2\psi_{BI}}\right)\end{aligned}$$

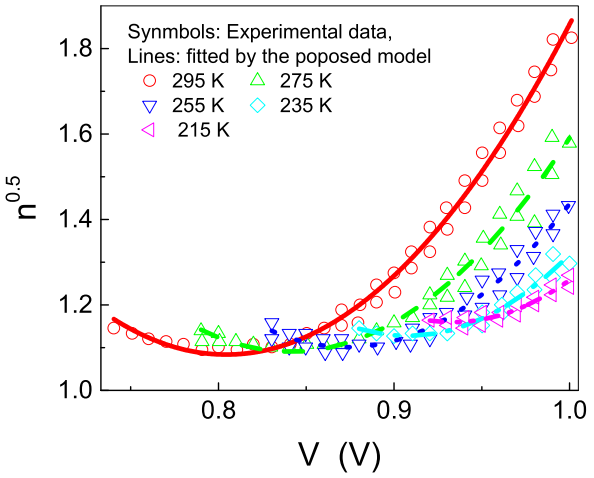

FIGURE 5. The square root of the ideality factor of organic semiconductor diodes as a function of the applied voltage across the depletion region under different temperatures. The experimental data from Ref. [1].

$$\begin{aligned}&= (1 + 1.5\mu\psi_{BI}) + \frac{\mu}{W_D\sqrt{\frac{2q\psi_{BI}}{m^*}}}(V - \psi_{BI}) \\ &\quad + \frac{\mu}{4\psi_{BI} W_D\sqrt{\frac{2q\psi_{BI}}{m^*}}}(V - \psi_{BI}) \quad (31)\end{aligned}$$

where m^* is effective carrier mass. Eq. 32 describes the dependent relationship between the ideality factor and the applied voltage when the mobility is weakly dependent on the applied voltage. Considering both the diagonal and off-diagonal disorders in the organic semiconductor, $\mu \sim e^{BF^{1/2}}$ and $\mu \sim \frac{1}{F} \sim \frac{1}{V}$ for completely drift controlled transport in organic semiconductor [11]. If $\mu = Ae^{BF^{1/2}}$ is assumed, Eq. 32 can be rewritten as

$$\begin{aligned}\sqrt{n} &\approx 1 + \mu_e \frac{V}{2\sqrt{\frac{4\varepsilon_s}{\psi_{BI} N_D m^*}}} \left(1 + \frac{V}{2\psi_{BI}}\right) \\ &= 1 + \frac{Ae^{BF^{1/2}} V}{2\sqrt{\frac{4\varepsilon_s}{\psi_{BI} N_D m^*}}} \left(1 + \frac{V}{2\psi_{BI}}\right) \\ &\approx 1 + \frac{A\left(1 + BV^{1/2}\right)V}{2\sqrt{\frac{4\varepsilon_s}{\psi_{BI} N_D m^*}}} \left(1 + \frac{V}{2\psi_{BI}}\right) \\ &= 1 + \frac{A}{2\sqrt{\frac{4\varepsilon_s}{\psi_{BI} N_D m^*}}} \left(1 + BV^{1/2} + \frac{V}{2\psi_{BI}} + \frac{BV^{3/2}}{2\psi_{BI}}\right) \quad (32)\end{aligned}$$

If that $\mu = \frac{A}{V}$ is assumed, Eq. 32 can be rewritten as

$$\begin{aligned}\sqrt{n_e} &\approx 1 + \mu \frac{V}{2\sqrt{\frac{4\varepsilon_s}{\psi_{BI} N_D m^*}}} \left(1 + \frac{V}{2\psi_{BI}}\right) \\ &= 1 + \frac{A}{2\sqrt{\frac{4\varepsilon_s}{\psi_{BI} N_D m^*}}} \left(1 + \frac{V}{2\psi_{BI}}\right) \quad (33)\end{aligned}$$

Lastly, the temperature-dependent effective barrier height in organic semiconductor diodes will be discussed, According to Eqs. 23 and Eq.27, the effective barrier height of

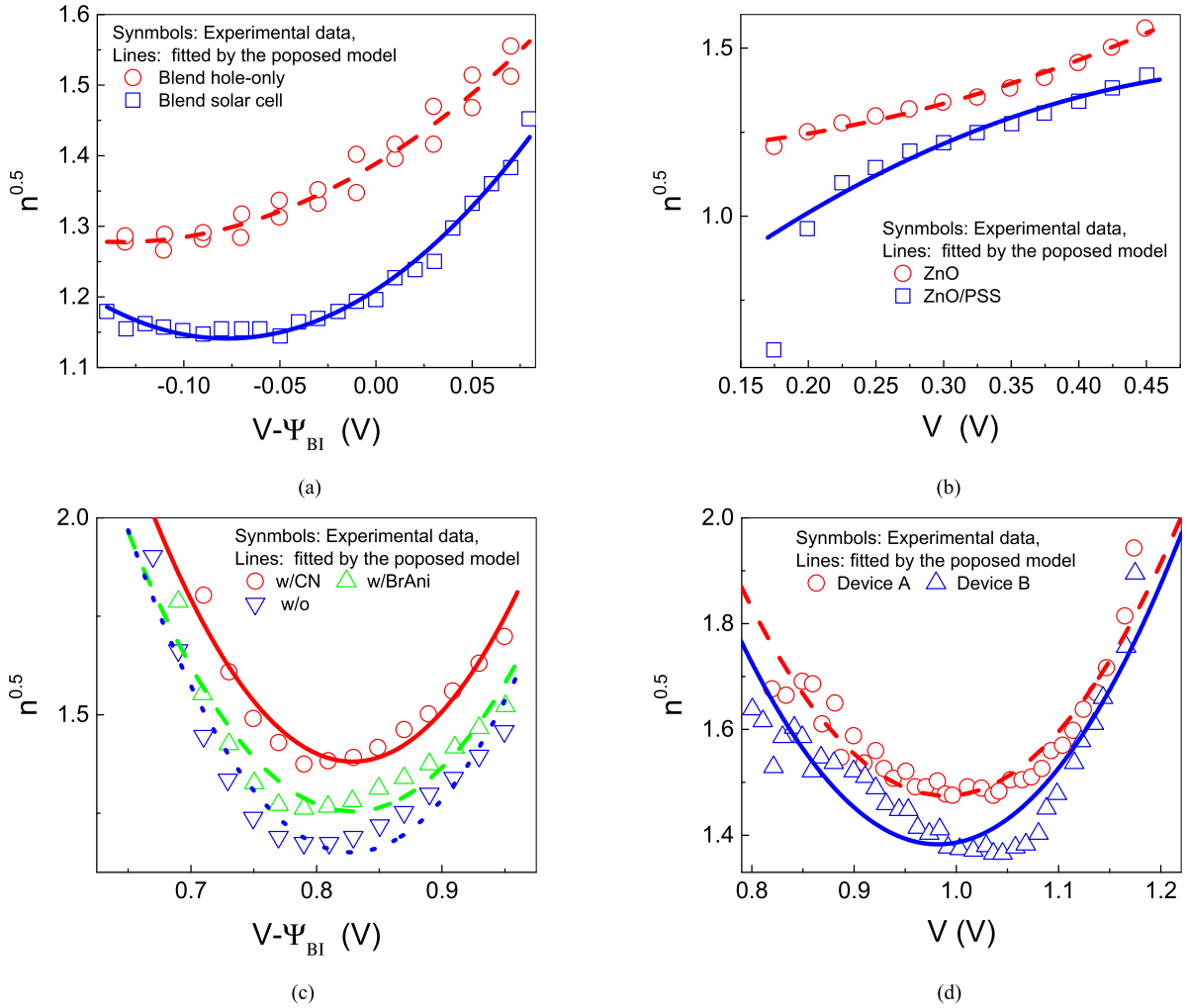

FIGURE 4. The square root of the ideality factor of organic semiconductor diodes as a function of the applied voltage across the depletion region. (a) the experimental data from Ref. [1], (b) the experimental data from Ref. [2], (c) the experimental from Ref. [3], (d) the experimental data from Ref. [4].

such organic semiconductor diode under one-order Taylor expansion is

$$\begin{aligned} q\phi_{BE} &= q\phi_n + \frac{q\left(\phi_m - \chi\right) - q\phi_n}{\left(1 + ET_L^{-\frac{3}{2}}\left(1 + \frac{1}{2}FT_L\right)\right)^2} \\ &= -k_B T_L \ln\frac{N_D}{N_C} + \left(q\left(\phi_m - \chi\right) + k_B T_L \ln\frac{N_D}{N_C}\right) \\ &\quad \times \left(1 - 2ET_L^{-\frac{3}{2}}\left(1 + \frac{1}{2}FT_L\right)\right) \\ &= q\left(\phi_m - \chi\right) - k_B \ln\frac{N_D}{N_C}\left(T_L\right)^{\frac{1}{2}} \\ &\quad - \left(q\left(\phi_m - \chi\right)EF + 2Ek_B \ln\frac{N_D}{N_C}\right)\left(T_L\right)^{-\frac{1}{2}} \\ &\quad - 2Eq\left(\phi_m - \chi\right)\left(T_L\right)^{-\frac{3}{2}} \end{aligned} \tag{34}$$

Thus, the temperature-dependent effective Schottky barrier height of such organic semiconductor diode can be conveyed by the equation

$$q\phi_{BE} \propto T^{\alpha} \tag{35}$$

where α is a parameter and $\alpha < 1$.

In the above discussion, the hot-carriers effects in organic semiconductor diodes whose current transport current is dominated by the band-like conduction mechanism on their performance have been analyzed. In the following, we will discuss how hot-carriers effects in organic semiconductor diodes whose current transport current is dominated by the hopping conduction mechanism impacts on their performance. For the case of organic semiconductor diodes under the hopping conduction mechanism, the density of states of an organic semiconductor can be described as a series of Gaussian profiles have been concluded from experiment [14], [15]:

$$dn_{OS} = N_{OS}\frac{1}{1 + \exp\left(\frac{E - E_F}{k_B T}\right)}$$

$$\times \frac{\exp\left(-\frac{(E+qV-E_{HOMO})^2}{2(\sigma_H)^2}\right)}{\sigma_H\sqrt{2\pi}}dE \tag{36}$$

$$dp_{OS} = N_{OS}\frac{1}{1+\exp\left(\frac{E-E_F}{k_BT}\right)} \times \frac{\exp\left(-\frac{(E+qV-E_{LUMO})^2}{2(\sigma_L)^2}\right)}{\sigma_L\sqrt{2\pi}}dE \tag{37}$$

where N_{OS} is the number of molecules of organic semiconductors, E_{HOMO} is the Gaussian peak centered at HOMO maximum with a standard deviation of σ_{H}, and E_{LUMO} is the Gaussian peak centered at LUMO maximum with a standard deviation of σ_{L}. The standard deviation for HOMO can be estimated from the full width at half maximum (FWHM) of experimental UPS [16] and inverse photoemission spectroscopy measurements [17]. In other words, a Gaussian type of the density of states of organic semiconductors is just an empirical conclusion or phenomenological conclusion. In the following, the phenomenological conclusion of organic diode current will be discussed and analyzed.

Considering the thermionic emission over the junction barrier and the density of states of an organic semiconductor, the current from the organic semiconductor to the metal can be written as

$$J_{\mathrm{OS}\to m} = \int_{E_{Fn}+q\phi_{Bn}}^{\infty} qv_i dN_{OS}\frac{1}{1+\exp\left(\frac{E-E_F}{k_BT}\right)} \times \frac{\exp\left(-\frac{(E+qV-E_{HOMO})^2}{2(\sigma_H)^2}\right)}{\sigma_H\sqrt{2\pi}}dE \tag{38}$$

$$J_{\mathrm{OS}\to m} = \int_{E_{Fn}+q\phi_{Bn}}^{\infty} qv_i d_{N_{OS}\frac{1}{1+\exp\left(\frac{E-E_F}{k_BT}\right)}\times OS} \times \frac{\exp\left(-\frac{(E+qV-E_{LUMO})^2}{2(\sigma_L)^2}\right)}{\sigma_L\sqrt{2\pi}}dE \tag{39}$$

Obviously, $v_i = v_x + v_{app}$. Here, v_{app} is the velocity caused by the applied voltage in the organic semiconductor. It is similar to the drift velocity for the case of the band-like conduction mechanism. Whether the current transport mechanism is the band-like conduction mechanism or the hopping conduction mechanism, the experimental data of the current through an organic semiconductor diode can be described by the thermionic emission over the barrier [1], [2], [4], [6], expressed by the standard diode equation [3], [5], [7], [8]. All these results imply that the experimental organic diode currents have a similar mathematical expression. This implies that integrating Eq. 39 and Eq. 40 will have a similar mathematical expression of a conventional organic semiconductor diode, that is

$$J_{OS\to M} \propto e^{-\frac{q\phi_n}{k_BT_L}}e^{-\frac{m_e^*v_{0x}^2}{2k_BT_L}} \tag{40}$$

If carriers in the organic semiconductors can not get additional energy from the applied electric field, the minimum velocity required in the transport direction to surmount the potential barrier region or the depletion region is given by $\frac{1}{2}m_e^*v_i^2 = \frac{1}{2}m_e^*v_{0x}^2 = q(\psi_{bi}-V)$ for electrons and $\frac{1}{2}m_h^*v_i^2 = \frac{1}{2}m_h^*v_{0x}^2 = q(\psi_{bi}-V)$ for holes energy, respectively. On the other hand, the minimum velocity required in the transport direction to surmount the potential barrier region or the depletion region will decrease when carriers get additional energy from the applied electric field. It becomes that $\frac{1}{2}m_e^*v_i^2 = \frac{1}{2}m_e^*n_ev_{0x}^2 = q(\psi_{bi}-V)$ and $\frac{1}{2}m_h^*v_i^2 = \frac{1}{2}m_h^*n_hv_{0x}^2 = q(\psi_{bi}-V)$ for electrons and holes, respectively. After carriers with additional energy from the applied electric field are considered, the organic diode current equation has the following form

$$J_{OS\to M} \propto e^{-\frac{\left(q\phi_n+\frac{q\psi_{bi}}{n}\right)}{k_BT_L}}e^{\frac{qV}{k_BT_Ln}} \tag{41}$$

where $\sqrt{n} = 1+\frac{\mu_eF_{ave}}{v_x}$ if the velocity caused by the applied voltage has been expressed as the same mathematical form as the drift velocity for the case of band-like transport.

In summary, for a metal-organic semiconductor junction and an inorganic semiconductor/organic semiconductor junction under the forward bias, the thermionic emission carriers are electrons in an n-type organic hole in a p-type organic semiconductor. In other words, there are no substantial current differences between a metal-organic semiconductor junction and an inorganic semiconductor/organic semiconductor junction when the carriers flow from the organic semiconductor into the metal or the inorganic semiconductor. Because there is no depletion region in the metal, it means that the hot-carriers effects in a metal/organic semiconductor junction when the carriers flow from the metal into the organic semiconductor under a forward bias could be neglected, whereas the hot-carriers effects in an inorganic semiconductor/n-type organic semiconductor junction, whether the carriers flow from the inorganic semiconductor into the organic semiconductor or from the organic semiconductor into the inorganic semiconductor under the forward bias, should be considered.

One should note that the validity of a scientific model can not be judged from whether the model itself is basic or simple. On the contrary, the problem-solving principle (Occam's razor) demonstrates that entities should not be multiplied without necessity. In this case, the one that requires the smallest number of assumptions is usually correct. A scientific model should be verified by the experimental results. Thus the proposed model will be compared with the experimental results.

III. RESULTS AND DISCUSSION

In the following calculation, the indium/rubrene single crystal diode has been chosen for the calculation. The barrier height at the indium/rubrene single-crystal interface is 1.0 eV (μ = 0.85 $\mathrm{cm^2V^{-1}s^{-1}}$, $\mathrm{N_A} = 2.47\times10^{14}$ $\mathrm{cm^{-3}}$, and $\mathrm{V_{BI}}$ = −0.66 V) [12], the dielectric constant of rubrene is 3 [13], and the effective hole mass in rubrene values from $0.65\mathrm{m_0}$ to 1.3 $\mathrm{m_0}$ ($\mathrm{m_0}$ is the free electron mass) [18].

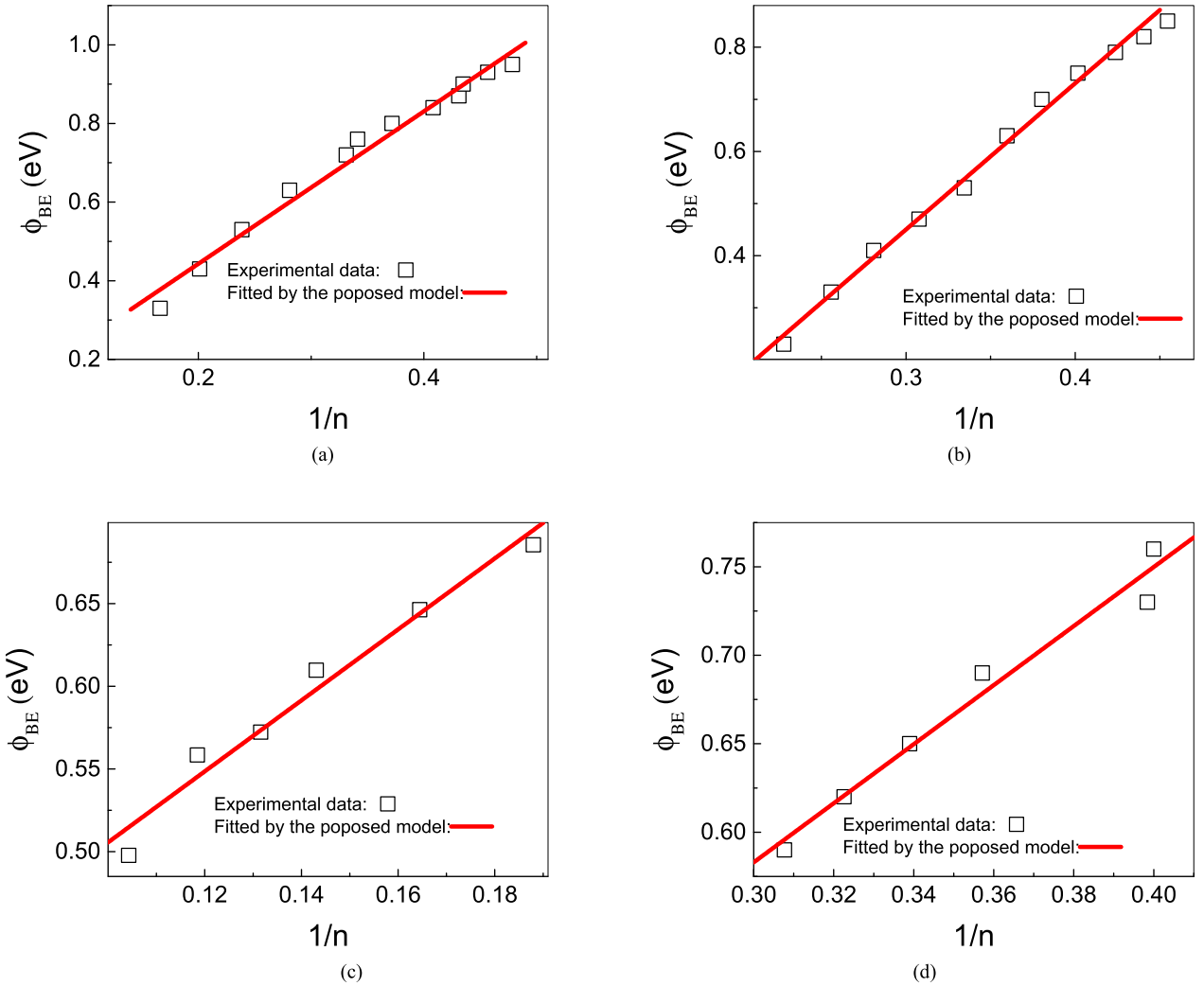

FIGURE 6. The comparison of the effective Schottky barrier height φ_{BE} of organic semiconductor diodes versus the reciprocal of the ideality factor $1/n$. (a) the experimental data from Ref. [5], (b) the experimental data from Ref. [6], (c) the experimental from Ref. [7], (d) the experimental data from Ref. [8].

Figure 2 depicts how the applied forward electric field and the hole concentration change with the position in the space-charge region of an indium/rubrene single crystal diode under different forward voltages. Figure 2a clearly shows that a negative electric field in the space-charge will be found when a forward voltage is applied to the diode. A negative electric field here means that holes will be accelerated along the negative x-direction. In other words, carriers become hot because they will get an additional drift velocity before overcoming the barrier at the indium/rubrene single-crystal interface from the applied forward electric field. This also represents that an accumulation region will appear in the space-charge region. Such an accumulation region can be easily found in Figure 2b. Figure 2b demonstrates that the accumulation region becomes more obvious when the applied forward voltage increases. These results imply that the carriers become hot before over the organic Schottky (junction) barrier under different forward voltages.

Figure 3 depicts how the applied forward electric field and the hole concentration change with the position in the space-charge region of an indium/rubrene single crystal diode at a given applied voltage under different acceptor densities. Figure 3a clearly shows that the negative electric field will be larger for a larger acceptor density at a given applied voltage. This means that carriers become hot at a given applied voltage from the applied electric field if the carrier mobility keeps the same. Figure 3b further support that there is an accumulation region when a forward voltage is applied to an indium/rubrene single crystal diode.

For the case of band-like conduction in organic semiconductor diodes, the square root of the ideality factor in the diode current equation of organic semiconductor diode dependence on the voltage can be described that $\sqrt{n} \propto C_0 + C_1 V + C_2 V^2$ according to Eq. 32. Here C_0, C_1, C_2 are fitting parameters. Figure 4 demonstrates that the proposed model can fit these experimental relations observed in organic

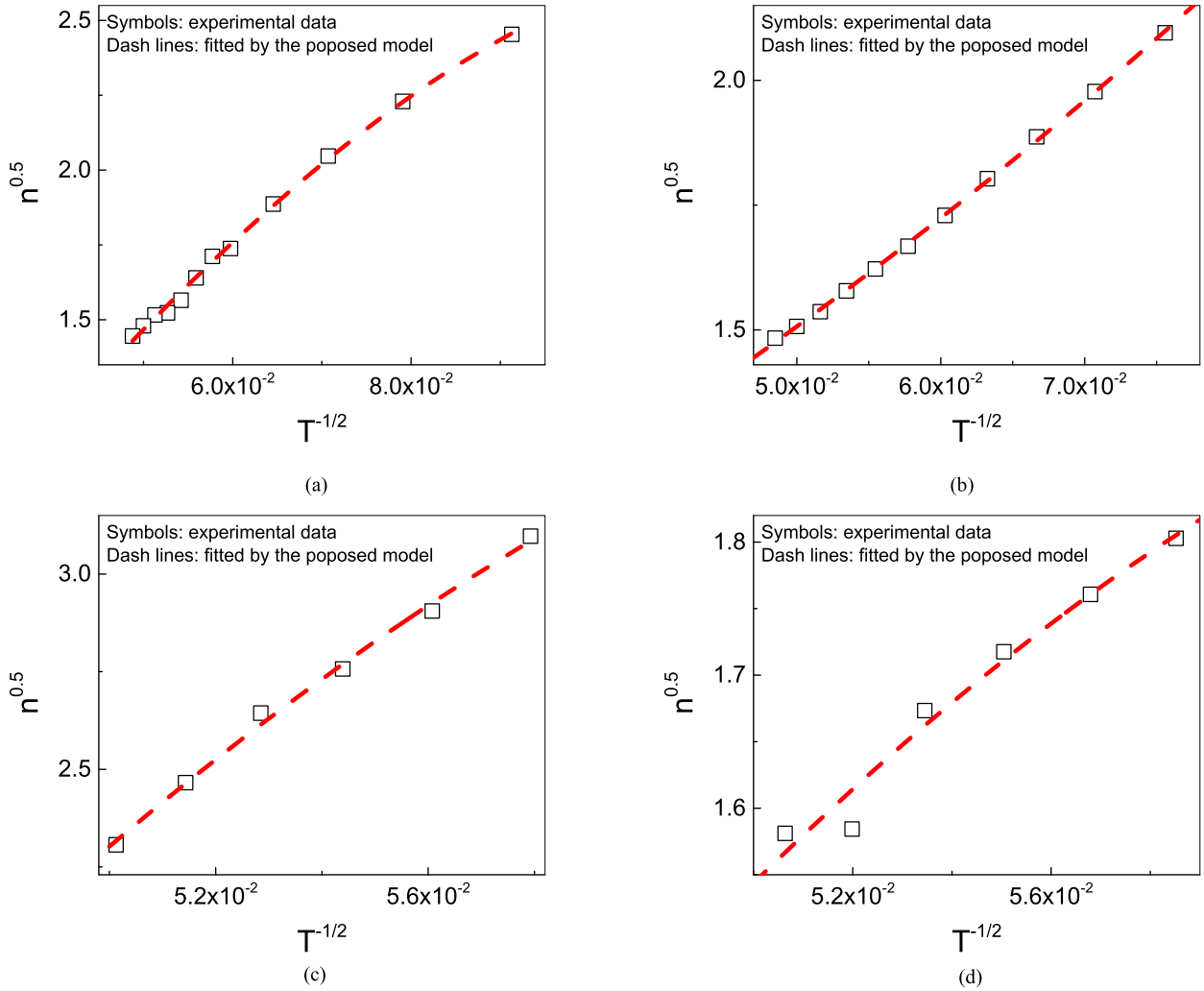

FIGURE 7. The comparison of $n^{0.5}$ versus $T^{-0.5}$ in organic semiconductor diodes. (a) the experimental data from Ref. [5], (b) the experimental data from Ref. [6], (c) the experimental from Ref. [7], (d) the experimental data from Ref. [8].

semiconductor diode very well. The data of Fig. 4a are from the polymer: fullerene bulk heterojunction solar cells [1]. The data of Fig. 4b are from the bulk heterojunction organic photodiodes with inverted device geometry and poly (styrenesulfonate) [2]. The data of Fig. 4c are from the P3HT:ICBA based polymer solar cells [3]. The data of Fig. 4d are from the perovskite solar cells [4].

Figure 5 further demonstrates that the proposed model is valid for describing the voltage-dependent ideality factor under different temperatures. These experimental relations between the ideality factor and voltage observed in organic semiconductor diodes under different temperatures can be fitted very well by the proposed model. The data of Fig. 5 are from the polymer: fullerene bulk heterojunction solar cells [1].

For the band-like conduction mechanism in organic semiconductors, the effective barrier height dependence on the ideality factor in organic semiconductor diodes can be described that $\phi_{BE} \propto \frac{1}{n}$ according to Eq. 23 and Eq. 24. Figure 6 shows how the effective barrier height ϕ_{BE} changes with the reciprocal of the ideality factor $1/n$ in organic semiconductor diodes. This figure clearly demonstrates that the experimental effective barrier height ϕ_{BE} versus the reciprocal of the ideality factor $1/n$ plots can be well described by using Eq. 27 for organic semiconductor diodes. The data of Fig. 6a are from the Au/PVC + TCNQ/p-Si Structures [5]. The data of Fig. 6b are from the polyvinyl Alcohol/n-InP Schottky diodes [6]. The data of Fig. 6c are from the Au/PoPDA/p-Si/Al heterojunction diodes [7]. the 6d are from the Au/TPP/p-Si/Al solar cells [8]. These results also prove that the proposed model is valid for modeling the organic semiconductor diodes.

For the band like conduction mechanism in organic semiconductors, the square root of the ideality factor dependence on the temperature in organic semiconductor diodes can be described that $\sqrt{n} \propto ET_L^{-\frac{1}{2}} + \frac{EF}{2}T_L^{-\frac{3}{2}}$ according to Eq. 27. Figure 7 depicts how the ideality factor of organic semiconductor diodes changes with temperature. It can be easily

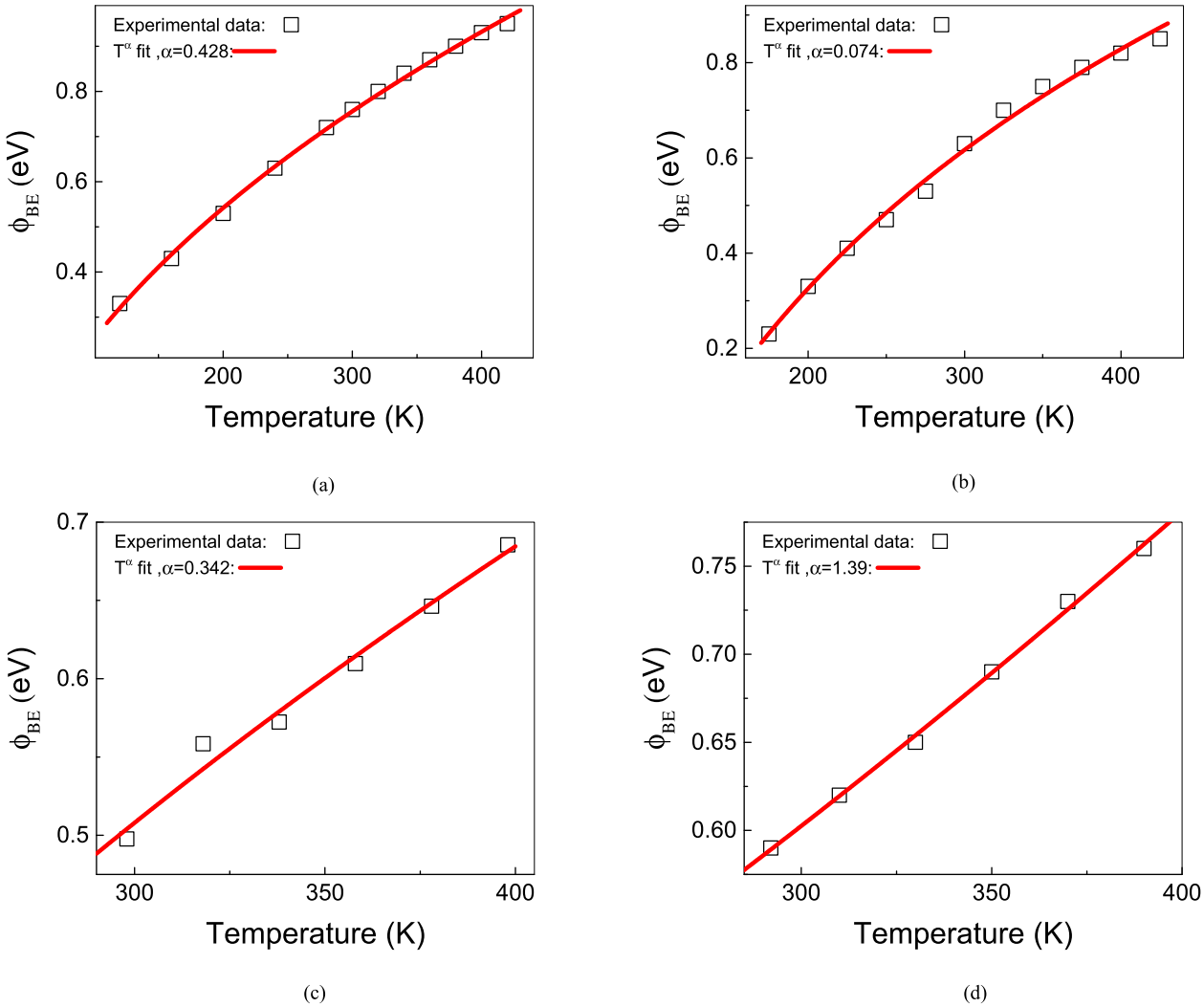

FIGURE 8. The comparison of the effective Schottky barrier height φ_{BE} of organic semiconductor diodes versus temperature. (a) the experimental data from Ref. [5], (b) the experimental data from Ref. [6], (c) the experimental from Ref. [7], (d) the experimental data from Ref. [8].

concluded from this figure that the proposed model ($\sqrt{n} \propto ET_L^{-\frac{1}{2}} + \frac{EF}{2}T_L^{-\frac{3}{2}}$) can describe the experimental data very well. The data of Fig. 7a are from the Au/PVC + TCNQ/p-Si Structures [5]. The data of Fig. 7b are from the polyvinyl Alcohol/n-InP Schottky diodes [6]. The data of Fig. 7c are from the Au/PoPDA/p-Si/Al heterojunction diodes [7]. The data of Fig. 7d are from the Au/TPP/p-Si/Al solar cells [8]. These results also prove that the proposed model is valid for modeling the organic semiconductor diodes.

For the band like conduction mechanism in organic semiconductors, the effective barrier height dependence on temperature in organic semiconductor diodes can be described that $q\phi_{BE} \propto T^{\alpha}$ according to Eq. 36. Figure 8 depicts how the effective barrier height in organic semiconductor diodes changes with temperature. It can be easily concluded from this figure that the proposed model ($q\phi_{BE} \propto T^{\alpha}$) can describe the experimental data observed in organic semiconductor diodes very well. The data of Fig. 8a are from the Au/PVC + TCNQ/p-Si Structures [5]. The data of Fig. 8b are from the polyvinyl Alcohol/n-InP Schottky diodes [6]. The data of Fig. 8c are from the Au/PoPDA/p-Si/Al heterojunction diodes [7]. The data of Fig. 8d are from the Au/TPP/p-Si/Al solar cells [8]. These results also prove that the proposed model is valid for modeling the organic semiconductor diodes.

In summary, one can note that the Schottky barrier should be a constant and the ideality factor should be 1 when there are no hot carrier effects in organic semiconductor diodes. Figure 2 and Figure 3 clearly show that the thermionic emission electrons can become hot because they will get an additional drift velocity before overcoming the barrier at the indium/rubrene single-crystal interface from the applied electric field. It can be concluded from both figures that the thermionic emission electrons become hotter for a larger applied voltage. In other words, the Schottky barrier height seen by hotter emission electrons should be reduced. It implies that there will be a dependent relationship between the Schottky barrier height and the applied voltage. Figures 6 and 8 demonstrate that the Schottky barrier height is

not constant and it depends on the applied voltage. Similarly, the ideality factor will depend on the applied voltage. Figures 4, 5 and 7 show that the ideality factor is not 1 and it depends on temperature. All these experimental results demonstrate that the experimental phenomena can originate from the hot-carrier effects in organic semiconductor diodes.

IV. CONCLUSION

Under parabolic band approximations (the band like conduction mechanism) or phenomenological analysis (the hopping conduction mechanism) on the organic semiconductor diodes, the impacts of the hot-carriers effects on the diode current in organic semiconductor diodes caused by the applied forward voltage on diode current have been physically modeled. The proposed model predicts that the hot-carriers effects can be a physical origin of the ideality factor and reduce the Schottky barrier height in the diode current equations of organic semiconductor diodes. The proposed model can describe the experimental diode current data of organic semiconductor diodes reported in the literature very well. At the same time, the comparison between the proposed model based on the band-like conduction mechanism in organic semiconductors and the experimental results shows that the model based on the band-like conduction mechanism is valid for modeling the performance of the organic semiconductor diodes. The physical origin of the ideality factor in the organic semiconductor diode current equation proposed in this paper provides a way of including the hot-carriers effects in the diode current equation. By comparing the results predicted by the proposed model with these experimental finds in organic semiconductors, it can be proved that such a model can describe the experimental diode current data of organic semiconductor diodes reported in the literature very well. Because the ideality factor or the effective Schottky barrier height in the diode current equation of organic semiconductor diodes is intuitively expressed that depends on the applied forward voltage, temperature, and the doping concentration, it is possible to accurate and physical modeling the effects of material parameters on the performance of organic semiconductor diodes. It can help us to physically understand the conduction mechanism in organic semiconductor-based devices that remains debated. It is also helpful for us to optimize the performance of organic semiconductor-based devices via tuning physical parameters.

REFERENCES

[1] G. A. H. Wetzelaer, M. Kuik, M. Lenes, and P. W. M. Blom, "Origin of the dark-current ideality factor in polymer: Fullerene bulk heterojunction solar cells," *Appl. Phys. Lett.*, vol. 99, no. 15, Oct. 2011, Art. no. 153506, doi: 10.1063/1.3651752.

[2] S. Yoon, J. Cho, K. M. Sim, J. Ha, and D. S. Chung, "Low dark current inverted organic photodiodes using anionic polyelectrolyte as a cathode interlayer," *Appl. Phys. Lett.*, vol. 110, no. 8, Feb. 2017, Art. no. 083301, doi: 10.1063/1.4977025.

[3] S. Yan, L. Lv, Y. Ning, L. Qin, C. Li, X. Liu, Y. Hu, Z. Lou, F. Teng, and Y. Hou, "Effects of solvent additives on trap-assisted recombination in P3HT: ICBA based polymer solar cells," *Phys. Status Solidi A*, vol. 212, no. 10, pp. 2169–2173, Oct. 2015, doi: 10.1002/pssa.201532250.

[4] P. Yadav, M. I. Dar, N. Arora, E. A. Alharbi, F. Giordano, S. M. Zakeeruddin, and M. Grätzel, "The role of rubidium in multiple-cation-based high-efficiency Perovskite solar cells," *Adv. Mater.*, vol. 29, no. 40, Oct. 2017, Art. no. 1701077, doi: 10.1002/adma.201701077.

[5] A. Kaya, S. Demirezen, H. Tecimer, and Ş. Altindal, "Temperature and voltage effect on barrier height and ideality factor in Au/PVC + TCNQ/p-Si structures," *Adv. Polym. Technol.*, vol. 33, no. 1, p. 21442, Dec. 2014, doi: 10.1002/adv.21442.

[6] M. S. P. Reddy, H.-S. Kang, J.-H. Lee, V. R. Reddy, and J.-S. Jang, "Electrical properties and the role of inhomogeneities at the polyvinyl alcohol/n-inp Schottky barrier interface," *J. Appl. Polym. Sci.*, vol. 131, no. 2, p. 39773, Jan. 2014, doi: 10.1002/APP.39773.

[7] M. S. Zoromba, M. H. Abdel-Aziz, M. Bassyouni, H. Bahaitham, and A. F. Al-Hossainy, "Poly(o-phenylenediamine) thin film for organic solar cell applications," *J. Solid State Electrochem.*, vol. 22, no. 12, pp. 3673–3687, Dec. 2018, doi: 10.1007/s10008-018-4077-x.

[8] M. M. Makhlouf and H. M. Zeyada, "Effect of annealing temperature and X-ray irradiation on the performance of tetraphenylporphyrin/p-type silicon hybrid solar cell," *Solid-State Electron.*, vol. 105, pp. 51–57, Mar. 2015, doi: 10.1016/j.sse.2014.11.020.

[9] S. Fratini and S. Ciuchi, "Bandlike motion and mobility saturation in organic molecular semiconductors," *Phys. Rev. Lett.*, vol. 103, no. 26, Dec. 2009, Art. no. 266601, doi: 10.1103/PhysRevLett.103.266601.

[10] V. Coropceanu, J. Cornil, D. A. da Silva Filho, Y. Olivier, R. Silbey, and J.-L. Brédas, "Charge transport in organic semiconductors," *Chem. Rev.*, vol. 107, no. 4, pp. 926–952, Apr. 2007, doi: 10.1021/cr050140x.

[11] P. Kumar, *Organic Solar Cells: Device Physics, Processing, Degradation, and Prevention*. New York, NY, USA: CRC Press. 2016, p. P162.

[12] T. Kaji, T. Takenobu, A. F. Morpurgo, and Y. Iwasa, "Organic single-crystal Schottky gate transistors," *Adv. Mater.*, vol. 21, no. 36, pp. 3689–3693, 2009, doi: 10.1002/adma.200900276.

[13] S. Fratini, A. F. Morpurgo, and S. Ciuchi, "Tuning electron-phonon and Coulomb interactions in organic field effect transistors," *Phys. Status Solidi C*, vol. 5, no. 3, pp. 718–721, 2008, doi: 10.1002/pssc.200777559.

[14] R. Jankowiak, K. D. Rockwitz, and H. Baessler, "Adsorption spectroscopy of amorphous Tetracene," *J. Phys. Chem.*, vol. 87, no. 4, pp. 552–557, Feb. 1983, doi: 10.1021/j100227a008.

[15] H. Bässler, "Charge transport in disordered organic photoconductors a Monte Carlo simulation study," *Phys. Status Solidi B*, vol. 175, no. 1, pp. 15–56, Jan. 1993, doi: 10.1002/pssb.2221750102.

[16] M. S. Khoshkhoo, H. Peisert, T. Chassé, and M. Scheele, "The role of the density of interface states in interfacial energy level alignment of PTCDA," *Organic Electron.*, vol. 49, pp. 249–254, Oct. 2017, doi: 10.1016/j.orgel.2017.06.065.

[17] D. R. T. Zahn, G. N. Gavrila, and M. Gorgoi, "The transport gap of organic semiconductors studied using the combination of direct and inverse photoemission," *Chem. Phys.*, vol. 325, no. 1, pp. 99–112, Jun. 2006, doi: 10.1016/j.chemphys.2006.02.003.

[18] J. Nitta, K. Miwa, N. Komiya, E. Annese, J. Fujii, S. Ono, and K. Sakamoto, "The actual electronic band structure of a rubrene single crystal," *Sci. Rep.*, vol. 9, no. 1, p. 9645, Dec. 2019, doi: 10.1038/s41598-019-46080-4.

[19] S. M. Sze and K. K. Ng, *Physics of Semiconductor Devices*. New York, NY, USA: Wiley, 2007.

[20] L.-F. Mao, H.-S. Ning, and J.-Y. Wang, "The current collapse in AlGaN/GaN high-electron mobility transistors can originate from the energy relaxation of channel electrons?" *PLoS ONE*, vol. 10, no. 6, Jun. 2015, Art. no. e0128438, doi: 10.1371/journal.pone.0128438.

[21] L.-F. Mao, "Current reduction caused by the quantum coupling of hot electrons in AlGaN/GaN transistors," *Phys. Status Solidi A*, vol. 215, no. 7, Apr. 2018, Art. no. 1701035, doi: 10.1002/pssa.201701035.

[22] L.-F. Mao, "Quantum coupling and electrothermal effects on electron transport in high-electron mobility transistors," *Pramana*, vol. 93, no. 1, p. 11, Jul. 2019, doi: 10.1007/s12043-019-1769-4.

[23] L. F. Mao, H. Ning, Z. L. Huo, and J. Y. Wang, "Physical modeling of gate-controlled Schottky barrier lowering of metal-graphene contacts in top-gated graphene field-effect transistors," *Sci. Rep.*, vol. 5, Dec. 2015, Art. no. 18307, doi: 10.1038/srep18307.

[24] L.-F. Mao, J. Wang, L. Li, H. Ning, and C. Hu, "Modeling of spectral shift in Raman spectroscopy, photo- and electro-luminescence induced by electric field tuning of graphene related electronic devices," *Carbon*, vol. 119, pp. 446–452, Aug. 2017, doi: 10.1016/j.carbon.2017.04.070.

[25] L.-F. Mao, "Thermionic emission current in graphene-based electronic devices," *Appl. Phys. A, Solids Surf.*, vol. 125, no. 5, p. 325, May 2019, doi: 10.1007/s00339-019-2627-4.
[26] L.-F. Mao, H. Ning, C. Hu, Z. Lu, and G. Wang, "Physical modeling of activation energy in organic semiconductor devices based on energy and momentum conservations," *Sci. Rep.*, vol. 6, no. 1, p. 24777, Jul. 2016, doi: 10.1038/srep24777.
[27] L.-F. Mao, "Impact of energy relaxation of channel electrons on drain-induced barrier lowering in nano-scale Si-based MOSFETs," *ETRI J.*, vol. 39, no. 2, pp. 284–291, Apr. 2017, doi: 10.4218/etrij.17.0116.0750.
[28] L.-F. Mao, "Temperature dependence of the tunneling current in metal-oxide-semiconductor devices due to the coupling between the longitudinal and transverse components of the electron thermal energy," *Appl. Phys. Lett.*, vol. 90, no. 18, Apr. 2007, Art. no. 183511, doi: 10.1063/1.2735929.
[29] L.-F. Mao, "The effects of the in-plane momentum on the quantization of nanometer metal-oxide-semiconductor devices due to the difference between the effective masses of silicon and gate oxide," *Appl. Phys. Lett.*, vol. 91, no. 12, Sep. 2007, Art. no. 123519, doi: 10.1063/1.2789733.
[30] L.-F. Mao, "The effects of the injection-channel velocity on the gate leakage current of nanoscale MOSFETs," *IEEE Electron Device Lett.*, vol. 28, no. 2, pp. 161–163, Feb. 2007, doi: 10.1109/LED.2006.889214.
[31] L.-F. Mao, "Investigation of the correlation between temperature and enhancement of electron tunneling current through HfO_2 gate stacks," *IEEE Trans. Electron Devices*, vol. 55, no. 3, pp. 782–788, Mar. 2008, doi: 10.1109/TED.2007.914471.
[32] L.-F. Mao, "Modeling the effects of the channel electron velocity on the channel surface potential of ballistic MOSFETs," *Solid-State Electron.*, vol. 52, no. 2, pp. 186–189, Feb. 2008, doi: 10.1016/j.sse.2007.11.008.
[33] L.-F. Mao, "Effects of channel electron in-plane velocity on the capacitance-voltage curve of MOS devices," *ETRI J.*, vol. 32, no. 1, pp. 68–72, Feb. 2010, doi: 10.4218/etrij.10.0109.0386.
[34] L.-F. Mao, "Effects of quantum coupling on the performance of metal-oxide-semiconductor field transistors," *Pramana*, vol. 72, no. 2, pp. 407–414, Feb. 2009, doi: 10.1007/s12043-009-0036-5.
[35] L.-F. Mao, "Physical model of the effects of drift velocity on current transport in PN junctions under the forward electric field," *Silicon*, pp. 1–17, Aug. 2019, doi: 10.1007/s12633-019-00249-8.

LING-FENG MAO received the Ph.D. degree in microelectronics and solid-state electronics from Peking University, Beijing, China, in 2001. He is currently a Professor with the School of Computer and Communication Engineering, University of Science and Technology Beijing, China. He has published over 170 research articles. His research interests include modeling and characterization of quantum effects in MOSFETs and semiconductors, characterization of quantum devices, fabrication, and modeling of integrated optic devices.